*Pharmaceutical Research, Vol. 8, No. 4, 1991*

*Research Article*

# Molecular Structure and Dynamics of *cis*(Z)- and *trans*(E)-Flupenthixol and Clopenthixol

**Ingebrigt Sylte[1,2] and Svein G. Dahl[1]**

*Received July 23, 1990; accepted November 10, 1990*

The three-dimensional structures and molecular electrostatic potentials of the *cis*(Z) and *trans*(E)-isomers of flupenthixol and clopenthixol were examined by computer graphics and molecular mechanical and quantum mechanical calculations, and their internal molecular motions were studied by molecular dynamics simulations *in vacuo* and in aqueous solution. The simulations demonstrated that both the side chains and the tricyclic ring systems of clopenthixol and flupenthixol are highly flexible. The angle between the two phenyl ring planes varied between 105 and 171° during the simulations in solution. The electrostatic potentials around the 2-substituent were significantly more negative in the *trans*(E)-isomers than in the *cis*(Z)-isomers. The stronger negative potentials may weaken electrostatic receptor interactions and, thereby, cause the *trans*(E)-isomers to be less active than *cis*(Z)-isomers. Differences both in three-dimensional structure and in electronic structure may cause the difference in pharmacological activity between *cis*(Z)- and *trans*(E)-thioxanthenes.

**KEY WORDS:** Thioxanthenes; *cis*(Z)- and *trans*(E)-isomers; molecular dynamics; conformations; molecular mechanics; electrostatic potentials.

## INTRODUCTION

The *cis*(Z)-isomers of several thioxanthene derivatives have antipsychotic effects, while the corresponding *trans*(E)-isomers are virtually inactive (1,2). The *cis*(Z)-isomers are also much more potent than the *trans*(E)-isomers in pharmacological tests related to antipsychotic activity (3–5) and in dopamine receptor binding experiments (5,6). *Cis*(Z)-thioxanthenes show high binding affinities to dopamine D1 and D2 receptors in the brain, and it has been questioned whether their antipsychotic action is mediated mainly via antagonism of central dopamine D2 receptors or by combined effects on D1 and D2 receptors (7).

Thioxanthene derivatives have a tricyclic ring system which is folded about the central S1–C9 axis (Fig. 1), an electron withdrawing substituent at the 2 position on the tricyclic nucleus, and a side chain with a nitrogen atom separated from the tricyclic nucleus by three carbon atoms. Both flupenthixol and clopenthixol have an *N*-hydroxyethylpiperazinyl group at the end of the side chain, and their only difference in chemical structure is that flupenthixol has a $CF_3$ group and clopenthixol a chlorine atom as 2 substituent (Fig. 1). Due to the exocyclic double bound (C9–C16) and the 2 substituent, the thioxanthenes may exist as *cis*(Z)- and as *trans*(E)-isomers. The molecular conformation of thioxanthenes may be described by the dihedral angles (D1–D3) of the side chain, the angle (α) between the two phenyl rings, and the distance (*d*) between nitrogen atom N1 in the side chain (Fig. 1) and the center of the substituted phenyl ring.

The detailed molecular mechanisms of interaction between thioxanthenes and dopamine receptors are not known. Dopamine has a *trans* extended conformation in crystals (8,9), and it has been suggested that the thioxanthenes mimic the three-dimensional *trans* conformation of dopamine in their interactions with dopamine receptors (10). Tollenaere *et al.* reported from crystallographic data and PCILO quantum chemical calculations that a good conformational fit could be obtained between *trans* dopamine and both the active and the inactive isomer of flupenthixol (11). Reboul and Cristau (12,13) compared geometrical parameters in crystal structures of dopamine receptor antagonists and concluded that the compounds had no common preferred conformation. Several other computational and crystallographic studies of dopamine receptor agonists and antagonists have since been performed in order to determine three-dimensional pharmacophoric patterns (14–18).

However, a limitation in the postulated pharmacophoric patterns may have been that previous studies of dopamine receptor ligands have been based upon fairly static concepts of molecular structure. The method of molecular dynamics simulations, which combines a molecular mechanical force field with Newton's equations of motion for a molecular system, has provided new insight into the molecular motions and functioning of biologically active molecules (19–21). This study examines the molecular dynamics, conformations, and molecular electrostatic potentials of the *cis*(Z)- and *trans*(E)-isomers of flupenthixol and clopenthixol, by

[1] Department of Pharmacology, Institute of Medical Biology, University of Tromsø, N-9001 Tromsø, Norway.
[2] To whom correspondence should be addressed.

0724-8741/91/0400-0462$06.50/0 

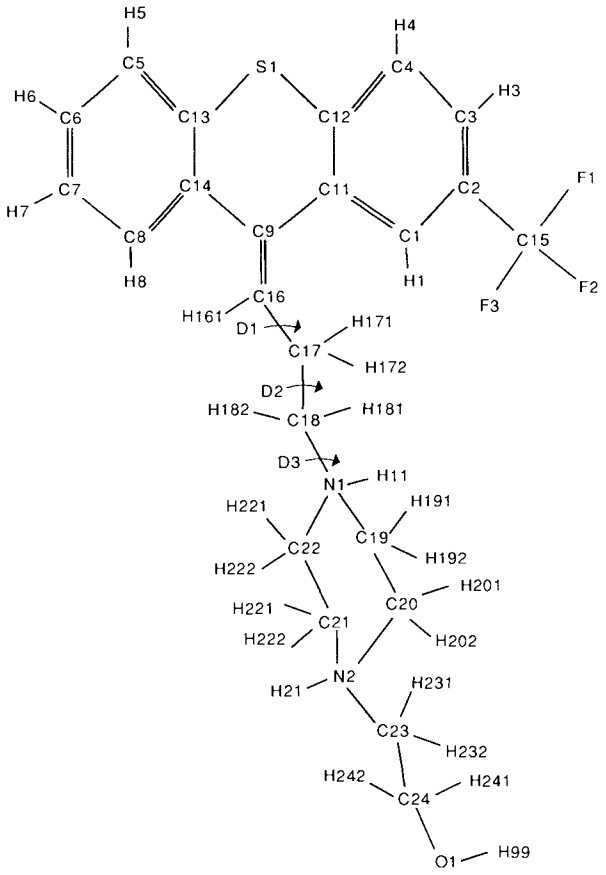


Fig. 1. Chemical structure and atom numbering scheme of flupenthixol. In clopenthixol the $CF_3$ group is replaced by chlorine atom Cl1; otherwise similar atom numbers were used. Dihedral angles: D1, C9–C16–C17–C18; D2, C16–C17–C18–N1; D3, C17–C18–N1–C19.

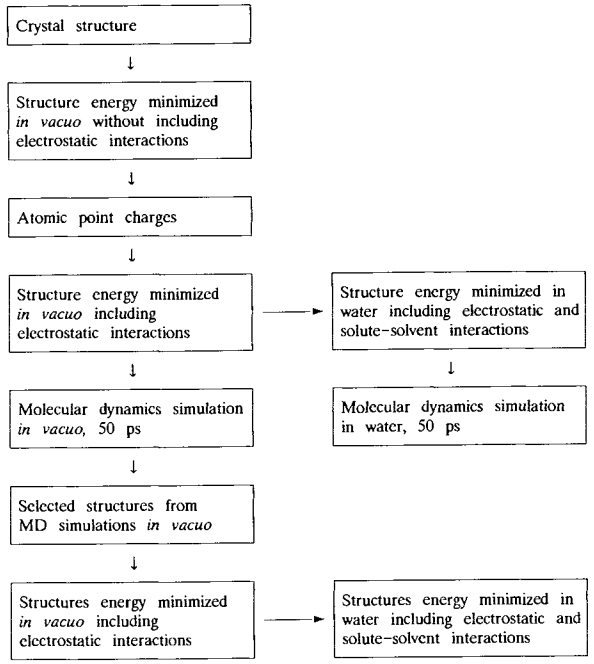


Fig. 2. Flow chart showing the molecular modeling procedure.

computer graphics and other computational techniques. The main purpose of our study was to explain the differences in pharmacological activities between *cis*(Z)- and *trans*(E)-thioxanthenes from their electronic and molecular structures and their molecular dynamics.

## METHODS

The subsequent steps of the molecular modeling procedure are shown in Fig. 2. Molecular mechanical geometry optimizations and molecular dynamics simulations were performed with the AMBER 3.0 programs (22–24), using the all atom force field and a 15-Å cutoff radius for nonbonded interactions. A distance-dependent dielectric function $\epsilon = r_{ij}$ ($r_{ij}$: interatomic distance) was used for electrostatic interactions *in vacuo*, and a constant dielectric function ($\epsilon = 1.0$) was used for electrostatic energies in the calculations with aqueous solvent. The calculations *in vacuo* were performed on a DEC VAX 8600/VMS computer. Molecular dynamics simulations in aqueous solution were performed on the VAX 8600 for the first 20 psec and on a Cray X/MP-28 computer for the following 30 psec.

Quantum mechanical atomic point charges were calculated with the QUEST 1.0 program (22,25) on a Cray X/MP-28 computer, using an STO-3G basis set. The QUEST program, which is supplied with the AMBER programs, is an extended GAUSSIAN-80 program (26) that calculates electrostatic potentials over several layers of molecular surfaces by *ab initio* quantum mechanical methods and projects the potentials into net atomic point charges by an optimization procedure. Electrostatic potentials were calculated over four surface layers 0.2 Å apart, the innermost surface corresponding to 1.4 times the van der Waals radii.

Molecular graphics was done with the MIDAS programs (27–29) on an Evans & Sutherland PS390 workstation with a DEC MicroVAX II/Ultrix system as the host machine. Water-accessible molecular surfaces (30) and electrostatic potentials 1.4 Å outside the surface were calculated with the MIDAS programs, using a 10-Å cutoff radius, and illustrated by color coding of the surfaces.

### Molecular Mechanical and Quantum Mechanical Calculations

The AMBER force field did not contain parameters for bond angles and torsion angles around the sulfur atom in the central thioxanthene ring. The following parameters were used: S–C bond—1.75 Å, 300 kcal $mol^{-1}$ $Å^{-2}$, from the crystal structure of di-p-tolyl sulfide (31); C–S–C angle—98.9°, 62 kcal $mol^{-1}$ $rad^{-2}$, from the microwave spectrum of dimethylsulfide (32); and torsion angle *X*–C–S–*X*, where *x* may be either H or C—1.8 kcal $mol^{-1}$, twofold barrier. The rotational barrier about the –C–S– torsion angle had previously been determined by quantum mechanical ab initio calculations, using the QUEST program, of the energies of thiophenol with the C–C–S–H torsion angle at different fixed positions (33).

Molecular mechanical energy minimizations were performed by the steepest descent method for 100 cycles, with

an initial step length of 0.05, followed by conjugate gradient minimization until convergence, which was reached with a $1.0 \times 10^{-7}$ kcal/mol energy difference or a gradient difference of 0.02 between subsequent steps.

The crystal structures of *cis*(Z)-flupenthixol (34), *trans*(E)-flupenthixol (35), and *cis*(Z)- and *trans*(E)-clopenthixol (36) were used as starting coordinates in the calculations. The crystal structure determinations had been performed with free bases, and since thioxanthenes are protonated at physiological pH (10), hydrogen atoms were added to the nitrogen atoms of the piperazine ring at standard distances and angles before further calculations were performed.

The protonated structures were initially refined by molecular mechanical energy minimization *in vacuo*, without including electrostatic interactions, and atomic point charges were calculated from this first set of refined structures. For computational reasons due to the size of the molecules, each molecule was divided into two overlapping fragments and the charges calculated for each fragment. A second set of structures was obtained by energy refinement *in vacuo* including electrostatic interactions. A layer of water with thickness 8 Å, containing approximately 240 randomly distributed water molecules, was added around each of these refined structures, and the solute–water systems were refined by molecular mechanical calculations including solute–solvent and electrostatic interactions.

### Molecular Dynamics Simulations

Starting coordinates for molecular dynamics simulations were obtained by molecular mechanical energy minimization of the crystal structures. Simulations without pressure monitoring and with conservation of total energy were performed for 50 psec at 300 K, with a step length of 0.001 psec, after 5 psec of initial equilibrium dynamics starting from 0.1 K. Bonds involving hydrogen were constrained using the Shake method. The nonbonded interaction list was updated every 50 steps during the simulations *in vacuo* and for the first 20 psec of the simulations in water and every 10 steps during the following 30-psec simulation in water. On the VAX 8600 computer a 50-psec simulation of flupenthixol *in vacuo* took 2 hr of CPU time and a 20-psec simulation of flupenthixol in water took 65 hr of CPU time. On the Cray X/MP-28 computer a 20-psec simulation of flupenthixol in water, with more frequent updating of the nonbonded interaction list, was done in 87 CPU min. The simulations with clopenthixol were slightly faster due to the smaller number of atoms.

The coordinates of the molecular system were saved to a disk file 100 times during each simulation *in vacuo*, 250 times during each simulation of a *cis*(Z)-isomer in aqueous solution, and 100 times during each simulation of a *trans*(E)-isomer in aqueous solution. The "Newton" module of the AMBER program package had been slightly modified such that the coordinates of water molecules were saved only for the initial and final coordinate sets, if desired.

The angle ($\alpha$) between the least-squares planes of the phenyl rings and the distance ($d$) between the center of the substituted phenyl ring and the nitrogen atom N1 of the side chain (Fig. 1) were calculated for each of the saved coordinate sets. Structures having different conformations, which were observed during the molecular dynamics simulation *in vacuo*, were selected and energy refined *in vacuo* and in aqueous solution as indicated in Fig. 2.

## RESULTS

### Molecular Conformation and Potential Energy

The relative energies, dihedral angles of the side chain, angle between the two phenyl rings, and distance between the center of the substituted phenyl ring and nitrogen atom N1 are given in Table I for clopenthixol and in Table II for flupenthixol. Structures 1 and 6 of clopenthixol were obtained by refinement of crystal structures and the other eight by refinement of structures from molecular dynamics simulations *in vacuo*. Structures 1 and 5 of flupenthixol were obtained by refinement of crystal structures and the other five from molecular dynamics simulations *in vacuo*.

The refined crystal structures of *cis*(Z)- and *trans*(E)-clopenthixol had highest energies among the conformations *in vacuo*, and the refined crystal structure of *trans*(E)-clopenthixol also had the highest energy in solution (Table I). The refined crystal structures of *cis*(Z)-flupenthixol and *trans*(E)-flupenthixol had slightly higher energies (0.1 and 0.9 kcal/mol) than the minimum energy conformations *in vacuo* (Table II). In aqueous solution the refined crystal structures of *cis*(Z)- and *trans*(E)-flupenthixol had 6.5–7.2 kcal/mol lower energies than the other conformations (Table II).

The energy difference between the minimum energy conformations of *cis*(Z)-clopenthixol was 5.8 kcal/mol *in vacuo* and 4.6 kcal/mol in aqueous solution, and the energy difference between the minimum energy conformations of *trans*(E)-clopenthixol was 8.5 kcal/mol *in vacuo* and 9.2 kcal/mol in aqueous solution (Table I). The *trans*(E)-isomers of both flupenthixol and clopenthixol had higher potential energies than the *cis*(Z)-isomers (Tables I and II). The energy differences between *cis*(Z)- and *trans*(E)-isomers were due mainly to intramolecular electrostatic interactions within the side chain, as shown in Table IV. The electrostatic interaction energies within the side chain were on average 2.4 kcal/mol higher *in vacuo* and 6.0 kcal/mol higher in solution for the *trans*(E)-isomers than for the *cis*(Z)-isomers of flupenthixol. For clopenthixol the intramolecular electrostatic interaction energies within the side chain were on average 3.6 kcal/mol higher *in vacuo* and 12.9 kcal/mol higher in solution for *trans*(E)-isomers than for the *cis*(Z)-isomers.

The electrostatic interaction energy between the positively charged piperazine ring and the 2 substituent was lower for *cis*(Z)-clopenthixol than for *trans*(E)-clopenthixol *in vacuo* and in aqueous solution and within similar ranges for *cis*(Z)-flupenthixol and *trans*(E)-flupenthixol (Table IV).

### Atomic Point Charges and Electronic Structure

The net atomic point charges were fairly similar for *cis*(Z)- and *trans*(E)-flupenthixol, except for atoms C8, C11, C14, C16, and C17 in the vicinity of the exocyclic double bond (Table V). The atomic point charges were also similar for *cis*(Z)- and *trans*(E)-clopenthixol, except for atoms C9, C11, C14, C16, and C17 around the exocyclic double bond.

Table I. Dihedral Angles (D1–D3) of the Side Chain, Angle (α) Between Least-Squares Planes of the Two Phenyl Rings, Distance (*d*) Between the Nitrogen Atom (N1) of the Side Chain and the Centroid of the Substituted Phenyl Ring, and Relative Molecular Mechanical Energies of Clopenthixol *in Vacuo* ($E_{vac}$) and in Aqueous Solution ($E_{wat}$)

| Str. No. | Config. | Phase[a] | Dihedral angle (deg) D1 | D2 | D3 | Plane angle α (°) | Atomic distance *d* (Å) | Relative energy (kcal/mol) $E_{vac}$ | $E_{wat}$ |
|---|---|---|---|---|---|---|---|---|---|
| 1 | *cis* | vac | 152.4 | 188.1 | 296.1 | 146.2 | 6.1 | 5.8 | |
| 2 | " | " | 132.8 | 307.8 | 296.4 | 144.2 | 5.4 | 4.6 | |
| 3 | " | " | 63.9 | 178.7 | 195.2 | 148.5 | 4.8 | 5.8 | |
| 4 | " | " | 146.3 | 306.2 | 295.3 | 143.7 | 5.8 | 0.0 | |
| 5 | " | " | 159.3 | 270.1 | 190.8 | 145.3 | 5.8 | 1.5 | |
| 1 | *cis* | wat | 149.3 | 191.1 | 302.5 | 149.6 | 6.1 | | 0.9 |
| 2 | " | " | 142.2 | 301.5 | 288.5 | 149.1 | 5.4 | | 2.7 |
| 3 | " | " | 63.0 | 183.9 | 201.8 | 156.3 | 4.8 | | 4.6 |
| 4 | " | " | 155.1 | 298.2 | 297.0 | 146.5 | 6.0 | | 3.8 |
| 5 | " | " | 150.3 | 276.5 | 190.8 | 152.4 | 5.7 | | 0.0 |
| 6 | *trans* | vac | 113.5 | 181.1 | 70.8 | 143.3 | 7.6 | 13.6 | |
| 7 | " | " | 207.7 | 184.8 | 170.7 | 145.0 | 7.6 | 6.5 | |
| 8 | " | " | 209.1 | 171.7 | 64.0 | 144.8 | 7.5 | 6.1 | |
| 9 | " | " | 298.8 | 134.4 | 68.2 | 142.0 | 6.9 | 7.1 | |
| 10 | " | " | 213.9 | 55.1 | 63.2 | 144.4 | 6.0 | 5.1 | |
| 6 | *trans* | wat | 111.4 | 174.4 | 64.3 | 143.8 | 7.5 | | 20.6 |
| 7 | " | " | 210.2 | 179.6 | 188.0 | 143.5 | 7.6 | | 11.9 |
| 8 | " | " | 210.2 | 182.0 | 71.1 | 147.0 | 7.6 | | 11.4 |
| 9 | " | " | 298.0 | 154.0 | 93.0 | 144.0 | 7.2 | | 16.3 |
| 10 | " | " | 220.4 | 35.1 | 53.2 | 160.0 | 5.4 | | 15.0 |

[a] vac, *in vacuo;* wat, in aqueous solution.

It is interesting to note, therefore, that as shown in Fig. 6, the electrostatic potentials of *cis*(Z)- and *trans*(E)-isomers were significantly different around the 2 substituent for both flupenthixol and clopenthixol. The lowest electrostatic potentials 1.4 Å outside the water accessible surface around the $CF_3$ group was −2.07 kcal/mol in *trans*(E)-flupenthixol and 3.01 kcal/mol in *cis*(Z)-flupenthixol. The lowest electrostatic potentials 1.4 Å outside the water accessible surface around the chlorine atom was −3.47 kcal/mol in *trans*(E)-clopenthixol and −0.74 kcal/mol in *cis*(Z)-clopenthixol.

## Molecular Dynamics Simulations

In the following the terms g (*gauche*), a (*anti*), and −g (−*gauche*) are used for dihedral angles in the ranges of 0–120, 120–240, and 240–360°, respectively. The molecular dy-

Table II. Dihedral Angles (D1–D3) of the Side Chain, Angle (α) Between Least-Squares Planes of the Two Phenyl Rings, Distance (*d*) Between the Nitrogen Atom (N1) of the Side Chain and the Centroid of the Substituted Phenyl Ring, and Relative Molecular Mechanical Energies of Flupenthixol *in Vacuo* ($E_{vac}$) and in Aqueous Solution ($E_{wat}$)

| Str. No. | Config. | Phase[a] | Dihedral angle (deg) D1 | D2 | D3 | Plane angle α (°) | Atomic distance *d* (Å) | Relative energy (kcal/mol) $E_{vac}$ | $E_{wat}$ |
|---|---|---|---|---|---|---|---|---|---|
| 1 | *cis* | vac | 244.7 | 174.0 | 287.2 | 143.3 | 5.7 | 0.1 | |
| 2 | " | " | 154.1 | 181.9 | 299.2 | 147.2 | 6.1 | 0.2 | |
| 3 | " | " | 152.2 | 170.7 | 60.8 | 147.4 | 6.1 | 0.1 | |
| 4 | " | " | 67.7 | 190.2 | 303.7 | 141.8 | 4.7 | 0.0 | |
| 1 | *cis* | wat | 148.5 | 178.9 | 314.8 | 140.4 | 5.6 | | 0.0 |
| 2 | " | " | 157.9 | 186.8 | 310.1 | 138.5 | 6.2 | | 10.0 |
| 3 | " | " | 152.0 | 168.2 | 57.7 | 136.2 | 6.2 | | 7.2 |
| 4 | " | " | 64.9 | 174.2 | 294.1 | 138.5 | 4.9 | | 10.5 |
| 5 | *trans* | vac | 208.7 | 301.7 | 301.8 | 145.9 | 6.4 | 3.9 | |
| 6 | " | " | 114.6 | 179.5 | 191.8 | 141.1 | 7.6 | 6.6 | |
| 7 | " | " | 211.5 | 52.1 | 185.3 | 145.4 | 5.9 | 3.0 | |
| 5 | *trans* | wat | 217.6 | 306.7 | 310.8 | 150.4 | 6.2 | | 10.8 |
| 6 | " | " | 103.3 | 179.9 | 167.4 | 148.6 | 7.4 | | 25.7 |
| 7 | " | " | 226.0 | 49.5 | 179.6 | 142.2 | 5.9 | | 17.3 |

[a] vac, *in vacuo;* wat, in aqueous solution.

namics simulations *in vacuo* and in aqueous solution demonstrated that both the side chains and the tricyclic ring systems of clopenthixol and flupenthixol are highly flexible, as shown in Figs. 3 and 4. The angle (α) between the phenyl rings ranged from 103 to 175° during the simulations *in vacuo* and from 105 to 171° during the simulations in aqueous solution (Table III). The angle between the phenyl rings was 146° and the distance between the nitrogen atom N1 and the substituted phenyl ring was 6.3 Å in the crystal structure of *cis*(Z)-clopenthixol (36). The corresponding mean values during the molecular dynamics simulation of *cis*(Z)-clopenthixol in aqueous solution were 143° and 6.1 Å (Table III). For *cis*(Z)-flupenthixol the corresponding angle and distance were 151° and 5.8 Å in the crystal structure (31) and, on average, 142° and 5.7 Å during the molecular dynamics simulation in aqueous solution (Table III).

Structure 1 of *cis*(Z)-clopenthixol, which had an a,a,−g conformation, was used as starting coordinates in the molecular dynamics simulation *in vacuo*. Already in the equilibrium phase the side chain changed to an a,−g,−g conformation which was retained for 16 psec. The following conformations were then observed: 16–32 psec g,a,a; 32–35 psec a,−g,−g; and 35–50 psec a,−g,a.

As may be noted from Table I, dihedral angles D1–D3 of the side chain had an a,−g,−g conformation in both structure 2 and structure 4 of *cis*(Z)-clopenthixol. However, the outer parts of the side chains had different conformations such that the side chain was folded over the ring system in structure no 2, while structure 4 had a more extended side chain, as shown in Fig. 5. The distance between the sulfur atom in the thioxanthene nucleus and the hydroxyl group at the end of the side chain stayed close to 2.7 Å during the initial 16 psec of the *in vacuo* simulation, when *cis*(Z)-clopenthixol conformations similar to that of structure 2 were observed.

**Fig. 3.** Superimposed molecular structures of *cis*(Z)-clopenthixol (above) and *trans*(E)-clopenthixol (below) observed during molecular dynamics simulations. Left: 33 structures observed at 1.5-psec intervals during 50-psec simulations *in vacuo*. Right: 33 structures observed at 1.5-psec intervals during 50-psec simulations in aqueous solution. Color coding of atoms: S, red; N, green; O, blue; Cl, yellow; C and H, white.

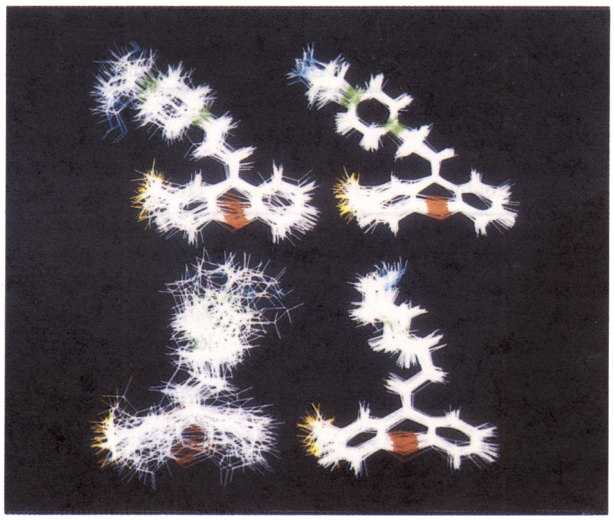

**Fig. 4.** Superimposed molecular structures of *cis*(Z)-flupenthixol (above) and *trans*(E)-flupenthixol (below) observed during molecular dynamics simulations. Left: 33 structures observed at 1.5-psec intervals during 50-psec simulations *in vacuo*. Right: 33 structures observed at 1.5-psec intervals during 50-psec simulations in aqueous solution. Color coding of atoms: S, red; N, green; O, blue; F, yellow; C and H, white.

Structure 6 (Table I) was used as starting coordinates in the molecular dynamics simulation of *trans*(E)-clopenthixol *in vacuo*. During the equilibrium phase the side chain shifted from a g,a,g to an a,a,a conformation, which was retained for the first 7 psec of the simulation, whereafter the following conformations were observed: 7–12 psec a,a,g; 12–20 psec −g,a,g; 20–35 psec a,g,g; 35–47 psec −g,a,g; and 47–50 psec a,g,g.

The molecular dynamics simulation of *cis*(Z)-flupenthixol *in vacuo* was started from structure 1, which had a −g,a,−g conformation (Table II). This conformation was retained throughout the equilibrium phase, and the following conformations were observed during the simulation: 0–21 psec −g,a,−g; 21–28 psec a,a,−g; 28–33 psec a,a,g; 33–41 psec a,a,−g; 41–50 psec g,a,−g.

The molecular dynamics simulation of *trans*(E)-flupenthixol *in vacuo* started from structure 5, which had an a,−g,−g conformation (Table II). This side-chain conformation was retained during the equilibrium phase and for the initial 2 psec of the simulation, and then the following conformations were observed: 2–15 psec g,a,a; 15–20 psec a,−g,−g; and 20–50 psec a,g,a.

The side-chain conformations of dihedral D1–D3 in the starting structures, −g,a,−g for *cis*(Z)-flupenthixol, a,−g,−g for *trans*(E)-flupenthixol, a,a,−g for *cis*(Z)-clopenthixol, and g,a,g for *trans*(E)-clopenthixol, were retained throughout the 5-psec equilibration periods and the subsequent 50 psec of molecular dynamics simulations in aqueous solution. As shown in Figs. 3 and 4, the molecular motions were somewhat dampened during the molecular dynamics simulations in aqueous solution, compared to the motions *in vacuo*. Nonbonded interactions with the 2 substituent caused the side chain of *trans*(E)-flupenthixol to stay close to the central C9–S1 axis during the simulations, and the side chain of the *cis*(Z)-isomer to be tilted toward the 2

**Table III.** Angle (α) Between Least-Squares Planes of the Two Phenyl Rings and Distance (*d*) Between the Centroid of the Substituted Phenyl Ring and Nitrogen Atom N1 in the Side Chain During Molecular Dynamics Simulations (MD) of Flupenthixol (FP) and Clopenthixol (CP)[a]

| | MD *in vacuo* | | MD in water | |
|---|---|---|---|---|
| Configuration | α (deg) | *d* (Å) | α (deg) | *d* (Å) |
| *cis*(Z)-CP | 103–170 (141) | 3.5–6.3 (5.3) | 123–167 (143) | 5.6–6.6 (6.1) |
| *trans*(E)-CP | 103–175 (139) | 5.4–7.7 (6.7) | 105–168 (143) | 7.1–7.8 (7.5) |
| *cis*(Z)-FP | 105–174 (140) | 4.4–6.6 (5.8) | 106–171 (142) | 5.2–6.2 (5.7) |
| *trans*(E)-FP | 104–174 (141) | 5.1–7.8 (6.5) | 114–168 (139) | 5.9–6.8 (6.4) |

[a] Observed range with mean value in parentheses.

substituent (Fig. 4). In both isomers the side chain was attracted to the $CF_3$ group by electrostatic interactions, but in *trans*(E)-flupenthixol a close contact was prevented by the rotational barrier about the exocyclic double bound.

The dihedral angle N2–C23–C24–O1 in the hydroxyethyl group of *cis*(Z)-flupenthixol shifted from a *gauche* to an *anti* conformation after 13.8 psec of the simulation in solution and remained in this conformation throughout the rest of the simulation. The hydroxyethyl group in *trans*(E)-flupenthixol remained in a *gauche* conformation, and the hydroxyethyl group in *trans*(E)-clopenthixol remained in an *anti* conformation, during the simulations in solution. The dihedral angle of the hydroxyethyl group in *cis*(Z)-clopenthixol shifted from a *−gauche* to an *anti* conformation after 7.4 psec and back to a *−gauche* conformation after 24 psec during the simulation in solution.

The piperazine ring at the side chan (Fig. 1) had a *chair* conformation in the crystal structures of *cis*(Z)- and *trans*(E)-isomers of clopenthixol and flupenthixol. The energy barrier for ring inversion of *N,N*-dimethylpiperazine was 13.3 kcal/mol (37), and the barrier for inversion of the piperazine ring in flupenthixol and clopenthixol is likely to be even higher due to the substituents on the nitrogen atoms. As expected, therefore, only *chair* conformations of the piperazine ring, with the amino hydrogens in axial positions, were observed during the simulations. The *chair* conformation of the piperazine ring in *trans*(E)-clopenthixol may be seen in the red-colored structure at the right in Fig. 5.

## DISCUSSION

In molecular dynamics simulations kinetic energy is added to the molecular system, in order to explore the nature of molecular motions across potential energy barriers between different low-energy conformations. It was expected, therefore, that various conformations of the side chain would be observed during the molecular dynamics simulations of clopenthixol and flupenthixol *in vacuo*, as shown in Figs. 3 and 4. It was not expected, however, that also the ring systems would move as much as they did during the simulations, the angle between the two phenyl rings ranging from 105 to 171° in solution and slightly more *in vacuo* (Table III). The flexibility of the molecules and the magnitude of molecular motions between different conformations during

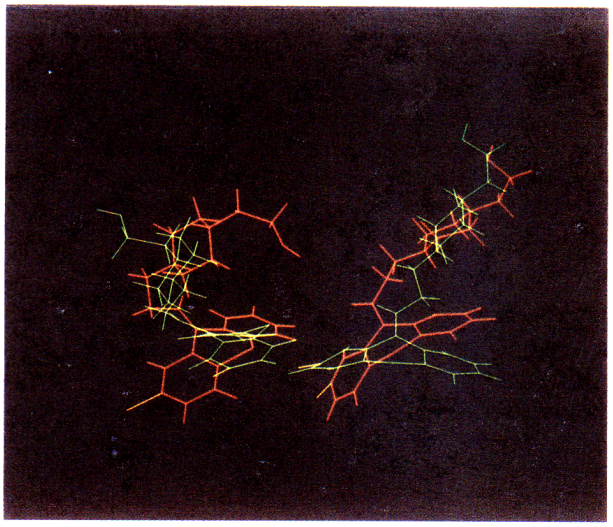

**Fig. 5.** Molecular structures of clopenthixol observed during molecular dynamics simulations *in vacuo*. Left: *cis*(Z)-clopenthixol. Red, a,−g,−g conformation (similar to structure 2) observed after 14 psec; green, a,−g,−g conformation (similar to structure 4) observed after 35 psec. Right: *trans*(E)-clopenthixol. Red, a,a,a conformation observed after 4 psec; green, −g,a,g conformation observed after 13 psec.

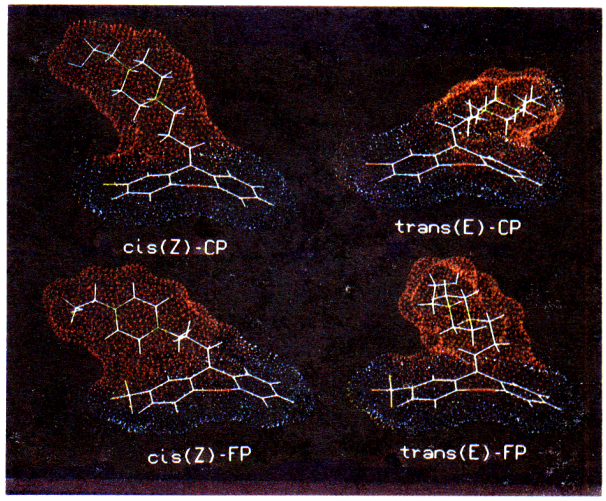


**Fig. 6.** Molecular structure and water-accessible surfaces of *cis*(Z)-clopenthixol (structure 1), *trans*(E)-clopenthixol (structure 6), *cis*(Z)-flupenthixol (structure 1), and *trans*(E)-flupenthixol (structure 5). CP, clopenthixol; FP, flupenthixol. Color coding of surfaces according to electrostatic potentials (*e*, kcal/mol): yellow, $e < 0$; blue, $0 \leq e < 12$; white, $12 \leq e < 15$; red, $e \geq 15$. Color coding of atoms as in Figs. 3 and 4.

Table IV. Nonbonded Interaction Energies (kcal/mol) of the Clopenthixol (CP) and Flupenthixol (FP) Structures Shown in Tables I and II[a]

| Compound | Str. no. | Configuration | $EEL_1$ | | $EEL_2$ | | vdW | |
|---|---|---|---|---|---|---|---|---|
| | | | $E_{vac}$ | $E_{wat}$ | $E_{vac}$ | $E_{wat}$ | $E_{vac}$ | $E_{wat}$ |
| CP | 1 | *cis*(Z) | 35.1 | 114.5 | −2.6 | −18.6 | −0.1 | −0.1 |
| | 2 | " | 32.4 | 110.6 | −2.0 | −15.9 | 0.0 | 0.0 |
| | 3 | " | 34.5 | 117.1 | −5.1 | −26.5 | −0.3 | −0.3 |
| | 4 | " | 28.0 | 114.4 | −1.9 | −15.3 | 0.0 | 0.0 |
| | 5 | " | 28.4 | 110.0 | −2.0 | −15.5 | 0.0 | 0.0 |
| | 6 | *trans*(E) | 41.4 | 132.1 | −1.2 | −12.2 | 0.0 | −0.1 |
| | 7 | " | 34.2 | 125.0 | −1.2 | −11.7 | 0.0 | 0.0 |
| | 8 | " | 34.1 | 124.6 | −1.2 | −12.0 | 0.0 | 0.0 |
| | 9 | " | 33.3 | 124.9 | −1.1 | −11.3 | 0.0 | 0.0 |
| | 10 | " | 33.0 | 124.5 | −1.8 | −18.6 | 0.0 | −0.1 |
| FP | 1 | *cis*(Z) | 31.4 | 121.1 | 0.0 | 5.4 | −0.1 | 0.0 |
| | 2 | " | 31.7 | 119.6 | 0.9 | 6.3 | −0.1 | −0.1 |
| | 3 | " | 31.8 | 118.0 | 0.8 | 5.7 | −0.1 | −0.1 |
| | 4 | " | 31.8 | 119.8 | 0.8 | 6.9 | −0.3 | −0.3 |
| | 5 | *trans*(E) | 33.9 | 127.7 | 0.9 | 7.0 | 0.0 | −0.1 |
| | 6 | " | 34.8 | 125.9 | 0.7 | 6.0 | −0.1 | 0.0 |
| | 7 | " | 33.6 | 123.3 | 1.2 | 8.0 | 0.0 | 0.0 |

[a] $EEL_1$, electrostatic interactions within the side chain; $EEL_2$, electrostatic interactions between the piperazine ring at the side chain and the 2 substituent on the ring system; vdW, van der Waals interactions between the piperazine ring and the 2 substituent; $E_{vac}$, energy *in vacuo*; $E_{wat}$, energy in aqueous solution.

the simulations clearly indicate that the receptor-bound conformations of *cis*(Z)-clopenthixol and *cis*(Z)-flupenthixol may be different from those having lowest energy *in vacuo* or in solution. A similar hypothesis has recently been postulated for the receptor bond conformation of acetylcholine (38).

The speed and magnitude of the molecular motions in the simulations show that in order to truly understand their mechanisms of action, their receptor interactions at the molecular level should be regarded as dynamic processes. As illustrated in Fig. 5, computer graphic visualization also showed that the motions between various conformations took place in a way that was quite different from what we had anticipated. Rather than rotating around single bonds while the rest of the molecule kept its shape, the conformational changes took place by twisting of the whole structure such that most of the mass was kept in place.

The flexibility of the thioxanthene ring systems during the simulations may be sensitive to the parameters used for bond angles and dihedral angles in the region of the S1 and C9 atoms. The fact that the average angle between the phenyl ring planes during the simulations agreed reasonably well with the crystal structures indicates that the parameters were appropriate. It is interesting to note that variations in the angle between phenyl ring planes of a similar magnitude, from 90 to 168°, were observed during simulations of four different tricyclic antidepressant drugs in aqueous solution, based on the supplied AMBER parameters only (39). These compounds have a central seven-membered ring with a dimethylene bridge where the thioxanthenes have a sulfur atom and a C–C double bond (in amitriptyline and nortriptyline) or an N–C single bond (in imipramine and chlorimipramine) as the exocyclic bond. From all this it seems that substantial variations in the folding of the tricyclic ring systems may be a general feature of the molecular dynamics of such drugs in aqueous solution.

The fact that the refined crystal structures of *cis*(Z)- and *trans*(E)-clopenthixol had the highest energies *in vacuo* demonstrates that molecular dynamics simulations may yield conformations with lower energies than those observed by X-ray crystallography. The refined crystal structures of flupenthixol did not have significantly higher energies than the other conformations. It is unlikely, therefore, that the higher energies of the refined crystal structures of *cis*(Z)- and *trans*(E)-clopenthixol were due to the force-field parameters that were used. It seems more likely that this was due to crystal packing forces, which have been demonstrated to increase the potential molecular mechanical energy of *cis*(Z)-chlorprothixene by 3.7 kcal/mol (40).

The differences between *cis*(Z)- and *trans*(E)-isomers in atomic point charges in the area of the exocyclic double bond were reflected in the different magnitudes of electrostatic interactions within the side chains (Table IV). This was the main reason for the lower molecular energies of the *cis*(Z)-isomers than of the *trans*(E)-isomers of clopenthixol and flupenthixol. Also, because the side chain lies closer to the 2 substituent in the *cis*(Z)-isomer than in the *trans*(E)-isomer, electrostatic interactions between the positively charged piperazine ring and the 2 substituent stabilized *cis*(Z)-clopenthixol more than *trans*(E)-clopenthixol. A similar difference in electrostatic interactions between the 2 substituent and the protonated dimethylamino group in the side chain has been found for *cis*(Z)- and *trans*(E)-chlorprothixene (40) but was not observed for the *cis*(Z)- and *trans*(E)-isomers flupenthixol (Table IV).

One of the most striking findings in this study was the difference between the *cis*(Z)- and *trans*(E)-isomers of clopenthixol and flupenthixol in electrostatic potentials around the 2 substituent (Fig. 6). This was due to the closer contact between the side chain and the 2 substituent in *cis*-isomers, where the positive charge of the protonated piperazine ring to a large extent neutralized the negative electrostatic poten-

Table V. Atomic Point Charges of *cis*(Z)- and *trans*(E)-Isomers of Clopenthixol (CP) and Flupenthixol (FP)[a]

| | Clopenthixol | | | Flupenthixol | | |
|---|---|---|---|---|---|---|
| Atom | *cis*(Z) | *trans*(E) | Diff | *cis*(Z) | *trans*(E) | Diff |
| C11 | −0.148 | −0.041 | −0.107 | 0.090 | 0.014 | 0.076 |
| C1 | −0.107 | −0.136 | 0.029 | −0.161 | −0.112 | −0.049 |
| H1 | 0.073 | 0.100 | −0.027 | 0.101 | 0.075 | 0.026 |
| C2 | 0.213 | 0.217 | −0.004 | −0.130 | −0.138 | 0.008 |
| Cl1 | −0.220 | −0.212 | −0.008 | | | |
| C15 | | | | 0.754 | 0.780 | −0.026 |
| F1 | | | | −0.220 | −0.230 | 0.010 |
| F2 | | | | −0.224 | −0.226 | 0.002 |
| F3 | | | | −0.240 | −0.240 | 0.000 |
| C3 | −0.095 | −0.101 | 0.006 | −0.083 | −0.070 | −0.013 |
| H3 | 0.110 | 0.107 | 0.003 | 0.093 | 0.089 | 0.004 |
| C4 | −0.157 | −0.137 | −0.020 | −0.058 | −0.081 | 0.023 |
| H4 | 0.111 | 0.106 | 0.005 | 0.081 | 0.084 | −0.003 |
| C12 | 0.238 | 0.173 | 0.065 | 0.106 | 0.141 | −0.035 |
| S1 | −0.126 | −0.117 | −0.009 | −0.098 | −0.101 | 0.003 |
| C13 | 0.132 | 0.085 | 0.047 | 0.093 | 0.058 | 0.035 |
| C5 | −0.094 | −0.081 | −0.013 | −0.067 | −0.058 | −0.009 |
| H5 | 0.087 | 0.087 | 0.000 | 0.080 | 0.083 | −0.003 |
| C6 | −0.071 | −0.084 | 0.013 | −0.090 | −0.094 | 0.004 |
| H6 | 0.082 | 0.085 | −0.003 | 0.086 | 0.087 | −0.001 |
| C7 | −0.040 | −0.045 | 0.005 | −0.041 | −0.020 | −0.021 |
| H7 | 0.070 | 0.068 | 0.002 | 0.072 | 0.068 | 0.004 |
| C8 | −0.135 | −0.170 | 0.035 | −0.142 | −0.218 | 0.076 |
| H8 | 0.074 | 0.079 | −0.005 | 0.085 | 0.103 | −0.018 |
| C9 | 0.152 | 0.017 | 0.135 | −0.044 | −0.015 | −0.029 |
| C14 | −0.015 | 0.093 | −0.108 | 0.058 | 0.130 | −0.072 |
| C16 | −0.304 | −0.149 | −0.155 | −0.156 | −0.102 | −0.054 |
| H161 | 0.117 | 0.085 | 0.032 | 0.097 | 0.045 | 0.052 |
| C17 | 0.178 | −0.016 | 0.194 | 0.009 | −0.190 | 0.199 |
| H171 | 0.004 | 0.061 | −0.057 | 0.051 | 0.133 | −0.082 |
| H172 | 0.050 | 0.068 | −0.018 | 0.043 | 0.090 | −0.047 |
| C18 | −0.203 | −0.210 | 0.007 | −0.203 | −0.210 | 0.007 |
| H181 | 0.119 | 0.145 | −0.026 | 0.119 | 0.145 | −0.026 |
| H182 | 0.116 | 0.149 | −0.033 | 0.116 | 0.149 | −0.033 |
| N1 | 0.296 | 0.302 | −0.006 | 0.296 | 0.302 | −0.006 |
| H11 | 0.234 | 0.233 | 0.001 | 0.234 | 0.234 | 0.000 |
| C19 | −0.091 | −0.091 | 0.000 | −0.091 | −0.091 | 0.000 |
| H191 | 0.067 | 0.067 | 0.000 | 0.067 | 0.067 | 0.000 |
| H192 | 0.152 | 0.152 | 0.000 | 0.152 | 0.152 | 0.000 |
| C22 | −0.073 | −0.073 | 0.000 | −0.073 | −0.073 | 0.000 |
| H221 | 0.178 | 0.178 | 0.000 | 0.178 | 0.178 | 0.000 |
| H222 | 0.117 | 0.117 | 0.000 | 0.116 | 0.116 | 0.000 |
| C21 | −0.412 | −0.412 | 0.000 | −0.413 | −0.413 | 0.000 |
| H211 | 0.178 | 0.178 | 0.000 | 0.178 | 0.178 | 0.000 |
| H212 | 0.177 | 0.177 | 0.000 | 0.177 | 0.177 | 0.000 |
| N2 | 0.672 | 0.672 | 0.000 | 0.672 | 0.672 | 0.000 |
| H21 | 0.188 | 0.188 | 0.000 | 0.188 | 0.188 | 0.000 |
| C20 | −0.202 | −0.202 | 0.000 | −0.202 | −0.202 | 0.000 |
| H201 | 0.103 | 0.103 | 0.000 | 0.103 | 0.103 | 0.000 |
| H202 | 0.165 | 0.165 | 0.000 | 0.165 | 0.165 | 0.000 |
| C23 | −0.386 | −0.386 | 0.000 | −0.387 | −0.387 | 0.000 |
| H231 | 0.157 | 0.157 | 0.000 | 0.157 | 0.157 | 0.000 |
| H232 | 0.172 | 0.172 | 0.000 | 0.172 | 0.172 | 0.000 |
| C24 | 0.222 | 0.222 | 0.000 | 0.222 | 0.222 | 0.000 |
| H241 | 0.073 | 0.073 | 0.000 | 0.073 | 0.073 | 0.000 |
| H242 | 0.011 | 0.011 | 0.000 | 0.011 | 0.011 | 0.000 |
| O1 | −0.534 | −0.534 | 0.000 | −0.534 | −0.534 | 0.000 |
| H99 | 0.359 | 0.359 | 0.000 | 0.359 | 0.359 | 0.000 |

[a] The numbering of atoms is shown in Fig. 1. Diff, difference between charge of *cis*(Z)- and charge of *trans*(E)-isomer.

tial created by the 2 substituent on the ring system. A similar difference in electrostatic potentials around the 2 substituent has been found for *cis*(Z)- and *trans*(E)-chlorprothixene (40), which indicates that this represents a general difference between *cis*(Z)- and *trans*(E)-thioxanthenes.

It has been suggested that the primary interaction of the protonated neuroleptic drug molecules with the dopamine D2 receptor is electrostatic, with a negatively charged residue at the active site (41,42). It seems likely that the negative molecular electrostatic potentials around the 2 substituent in *trans*(E)-thioxanthenes may weaken such electrostatic interactions and, thereby, cause these isomers to be less active than the *cis*(Z)-isomers in dopamine receptor binding and related tests. It is also possible that the differences in molecular shape between *cis*(Z)- and *trans*(E)-isomers, which are illustrated in Figs. 3 and 4, prevent a sufficiently strong complementary binding of *trans*(E)-isomers to the receptor. Differences both in three-dimensional structure and dynamics and in molecular electrostatic potentials may therefore explain why *trans*(E)-thioxanthenes have so much lower pharmacological activities than the *cis*(Z)-isomers.

## ACKNOWLEDGMENTS

This work was supported by grants from Troms Fylkeskommune and the Norwegian Research Council for Science and the Humanities (NAVF).

## REFERENCES

1. A. Gravem, E. Engstrand, and R. J. Guleng. Cis(Z)-clopenthixol and clopenthixol (Sordinol) in chronic psychotic patients. *Acta Psychiat. Scand.* 58:384–388 (1978).
2. E. C. Johnstone, T. J. Crow, C. D. Frith, M. W. P. Carney, and J. S. Price. Mechanism of the antipsychotic effect in the treatment of acute schizophrenia. *Lancet* 1:848–851 (1978).
3. R. J. Miller, A. A. Horn, and L. L. Iversen. The action of neuroleptic drugs on dopamine-stimulated adenosine cyclic 3′,5′-monophosphate production in rat neostriatum. *Mol. Pharmacol.* 10:759–766 (1974).
4. P. V. Petersen, I. Møller Nielsen, V. Pedersen, A. Jørgensen, and N. Lassen. In E. Usdin and I. S. Forrest (eds.), *Psychotherapeutic Drugs, Part 2. Applications*, Psychopharmacology Series 2, Marcel Dekker, New York, 1977, pp. 827–867.
5. J. Hyttel, J. Arnt, and K. P. Bogesø. In D. F. Smith (ed.), *CRC Handbook of Stereoisomers: Drugs in Psychopharmacology*, CRS Press, Boca Raton, Fla., 1984, pp. 143–214.
6. J. Hyttel and J. Arnt. Characterization of binding of $^3$H-SCH23390 to dopamine D-1 receptors. Correlation to other D-1 and D-2 measures and effect of selective lesions. *J. Neural. Transm.* 68:171–189 (1987).
7. J. Hyttel, J. Arnt, and M. van den Berghe. In S. G. Dahl and L. F. Gram (eds.), *Clinical Pharmacology in Psychiatry. From Molecular Studies to Clinical Reality*, Psychopharmacology Series 7, Springer-Verlag, Berlin, Heidelberg, 1989, pp. 109–122.
8. R. Bergin and D. Carlstrom. The structure of the catecholamines. II. The crystal structure of dopamine hydrochloride. *Acta Cryst.* B24:1506–1510 (1968).
9. J. Giesecke. Refinement of the structure of dopamine hydrochloride. *Acta Cryst.* B36:178–181 (1980).
10. A. S. Horn, M. L. Post, and O. Kennard. Dopamine receptor blockade and the neuroleptics, a crystallographic study. *J. Pharm. Pharmacol.* 27:553–563 (1975).
11. J. P. Tollenaere, H. Moereels, and M. H. Koch. On the conformation of neuroleptic drugs in the three aggregation state and their conformational resemblance to dopamine. *Eur. J. Med. Chem.* 12:199–211 (1977).

12. J. P. Reboul and B. Cristau. Analyse pharmacochimique des données fournies par la radiocristallographie des amines psychotropes polycycliques. I. Définition et calcul des paramètres conformationnels. *Eur. J. Med. Chem.* 12:71–75 (1977).
13. J. P. Reboul and B. Cristau. Analyse pharmacochimique des données fournies par la radiocristallographie des amines psychotropes polycycliques. II. Confrontation des valeurs paramètriques. *Eur. J. Med. Chem.* 12:76–79 (1977).
14. P. S. Seeman, M. Watnabe, D. Grigoriadias, J. L. Tedesco, S. R. George, U. Svensson, J. L. G. Nilsson, and J. L. Neumeyer. Dopamine $D_2$ receptor binding sites for agonists. A tetrahedral model. *Mol. Pharmacol.* 28:391–399 (1985).
15. A. A. Asselin, L. G. Humber, K. Voith, and G. Metcalf. Drug design via pharmacophore identification. Dopaminergic activity of $^3$H-benz[e]indol-8-amines and their mode of interaction with the dopamine receptor. *J. Med. Chem.* 29:648–654 (1986).
16. M. Froimowitz, J. L. Neumeyer, and R. J. Baldessarini. A stereochemical explanation of the dopamine agonist and antagonist activity of stereoisomeric pairs. *J. Med. Chem.* 29:1570–1573 (1986).
17. H. Van de Waterbeemd, P. A. Carrupt, and B. Testa. Similarities of pharmacophoric patterns revealed by the MEP of metoclopramide, molindone and piquindone, a subgroup of dopamine D-2 receptor agonists. *J. Mol. Graphics* 4:51–55 (1986).
18. D. T. Manallack and P. M. Beart. A three dimensional receptor model of the dopamine D2 receptor from computer graphic analyses of D2 agonists. *J. Pharm. Pharmacol.* 40:422–428 (1987).
19. Van W. F. Gunsteren and H. J. C. Berendsen. Algorithms for macromolecular dynamics and constraint dynamics. *Mol. Phys.* 34:1311–1327 (1977).
20. M. Karplus and J. A. McCammon. Dynamics of proteins: Elements and function. *Annu. Rev. Biochem.* 53:263–300 (1983).
21. J. W. Saldanha, B. Howlin, L. Du Toit, and R. A. Palmer. The dynamics of gallamine: A potent neuromuscular blocker. A determination by quantum mechanics and molecular dynamics. I. *In vacuo* studies. *J. Comp. Chem.* 10:975–981 (1989).
22. U. C. Singh, P. K. Weiner, J. W. Caldwell, and P. A. Kollman. *Assisted Model Building with Energy Refinement,* AMBER UCSF Version 3.0, Department of Pharmaceutical Chemistry, University of California, San Francisco, 1986.
23. S. J. Weiner, P. A. Kollman, D. A. Case, U. C. Singh, C. Ghio, G. Alagona, S. Profeta Jr., and P. Weiner. A new force field for molecular mechanical simulation of nucleic acids and proteins. *J. Am. Chem. Soc.* 106:765–784 (1984).
24. S. J. Weiner, P. A. Kollman, D. T. Nguyen, and D. A. Case. An all atom force field for simulations of proteins and nucleic acids. *J. Comp. Chem.* 7:230–252 (1986).
25. U. C. Singh and P. A. Kollman. An approach to computing electrostatic charges for molecules. *J. Comp. Chem.* 5:129–145 (1984).
26. J. S. Binkley, R. A. Whiteside, R. Kirshnan, R. Seeger, D. J. Derfress, H. B. Schlegel, S. Topiol, L. R. Kahn, and J. A. Pople. *GAUSSIAN 80, Quantum Chemistry Program Exchange,* 1980.
27. P. A. Bash, N. Pattabiraman, C. Huang, T. E. Ferrin, and R. Langridge. Van der Waals surfaces in molecular modeling: implementation with real-time computer graphics. *Science* 222: 1325–1327 (1983).
28. T. E. Ferrin, C. C. Huang, L. E. Jarvis, and R. Langridge. The MIDAS database system. *J. Mol. Graph.* 6:1–12 (1988).
29. T. E. Ferrin, C. C. Huang, L. E. Jarvis, and R. Langridge. The MIDAS display system. *J. Mol. Graph.* 6:13–27 (1988).
30. M. L. Connolly. Solvent-accessible surfaces of proteins and nucleic acids. *Science* 221:709–713 (1983).
31. W. R. Blackmore and S. C. Abrahams. Di-p-tolyl sulfide. *Acta Cryst.* 8:329–225 (1955).
32. L. Pierce and M. Hayashi. Microwave spectrum, dipole moment, structure, and internal rotation of dimethyl sulfide. *J. Chem. Phys.* 35:479–485 (1961).
33. S. G. Dahl, P. A. Kollman, S. N. Rao, and U. C. Singh. Unpublished results.
34. M. L. Post, O. Kennard, G. M. Sheldrick, and A. S. Horn. α-Flupenthixol. *Acta Cryst.* B31:2366–2368 (1975).
35. M. L. Post, O. Kennard, and A. S. Horn. β-Flupenthixol. *Acta Cryst.* B31:2724–2726 (1975).
36. P. G. Jones, G. M. Sheldrick, and A. S. Horn. Structures of the neuroleptic drugs α- and β-clopenthixol. *Acta Cryst.* B37:906–910 (1981).
37. J. Dahle. *Stereokjemi og konformasjonsanalyse* (Stereochemistry and conformational analysis), Universitetsforlaget, Oslo, 1975.
38. R. W. Behling, T. Yamane, G. Navon, and L. W. Jelinski. Conformation of acetylcholine bound to the nicotinic acetylcholine receptor. *Proc. Natl. Acad. Sci. USA* 85:6721–6725 (1985).
39. E. Heimstad, Ø. Edvardsen, T. E. Ferrin, and S. G. Dahl. Three dimensional structure and molecular dynamics of tricyclic antidepressants (submitted for publication).
40. I. Sylte and S. G. Dahl. Three dimensional structure and molecular dynamics of *cis*(Z)- and *trans*(E)-chlorprothixene. *J. Pharm. Sci.* (in press).
41. S. G. Dahl, Ø. Edvardsen, and I. Sylte. Molecular structure and dynamics of the dopamine $D_2$ receptor and ligands. *Clin. Neuropharmacol.* 13 (Suppl. 2):41–42 (1990).
42. P. G. Strange. Aspects of the structure of the $D_2$ dopamine receptor. *TINS* 13:373–378 (1990).